Proceedings of the 21st International Conference on Global Research and Education (Inter-Academia 2024)

Trajectory Tracking Control of Robot Manipulator Using Hybrid Control Strategy

A. Teklu[a] and J. Mozaryn[b,*]

[a] *Faculty of Mechatronics, Institute of Micromechanics and Photonics, Warsaw University of Technology, św. A. Boboli 8, 02-525 Warsaw, Poland*
[b] *Faculty of Mechatronics, Institute of Automatic Control and Robotics, Warsaw University of Technology, św. A. Boboli 8, 02-525 Warsaw, Poland*

Doi: 10.12693/APhysPolA.146.430 *e-mail: jakub.mozaryn@pw.edu.pl

This article proposes a linear–quadratic regulator-based optimal second-order sliding mode controller for trajectory tracking control of robot manipulators under lumped disturbance. The coupled dynamics of the manipulator with a geared motor and the desired joint space trajectory are designed and discussed. The linear–quadratic regulator controller is developed by penalizing corresponding weighting matrices for the nominal input–output linearized robot dynamics. An integral sliding mode control law is incorporated to address external disturbances, ensuring the linear–quadratic regulator's optimized performance remains unaffected. A non-singular terminal sliding mode control law is then cascaded with the optimal integral switching manifold to alleviate chattering effects. The proposed strategy, validated using SimMechanics™/Simulink in MATLAB®, demonstrates superior performance compared to known control algorithms by achieving joint trajectories with lower torque and smoother control. The validation of the proposed controller is based solely on simulation and has not been implemented practically. Specifically, the energy consumption and tracking errors of the proposed controller are 27.63 J and 0.00167, respectively.

topics: motor selection, robot, optimal control, second-order sliding mode control

1. Introduction

Robot manipulators are *multi-input multi-output* (MIMO) electromechanical systems that are highly nonlinear, dynamically connected among the joints, and resemble human arms [1–3]. Nowadays, industrial robots have taken over a wide range of human duties in various industries, including manufacturing and agriculture, to automate various operations. It is owing to the robots' hereditary qualities, such as the fact that they do not suffer fatigue, boredom, or any other circumstance that would prevent them from completing predetermined goals [1]. Robotic manipulators are frequently installed in industrial manufacturing to improve productivity, quality, and quantity of products and fulfill customer needs due to their capabilities of performing various tasks, such as arc welding, pick and place, painting, and assembly, unconditionally, as industries play an irreplaceable role in the economic growth of any country [2, 3].

Controlling an industrial manipulator reliably and precisely in the workplace is critical for completing activities that need high accuracy and repeatability while minimizing effect perturbations. However, designing a prominent controller for a robot manipulator is a difficult task because it necessitates working with inherently nonlinear and highly coupled dynamic equations, and the working environment is subjected to various external disturbances [4–8].

Various control strategies have been developed over time, including *feedback linearization* (FLC), *sliding mode control* (SMC), and optimal control, each with its advantages and limitations [9].

FLC is widely used to linearize and decouple nonlinear systems, enabling the application of linear control techniques. However, its effectiveness depends on an accurate system model. SMC, known for robustness and precision, guides system states onto a sliding manifold, but it often suffers from chattering — a rapid oscillation in control input — leading to wear and instability. Methods like integral sliding mode control (ISMC) and *second-order sliding mode control* (SOSMC) have been proposed to address chattering, although they can increase energy consumption.

This thesis proposes a novel *optimal second-order sliding mode control* (OSOSMC) that integrates SOSMC with a *linear–quadratic regulator* (LQR)-based optimal control. This hybrid approach aims

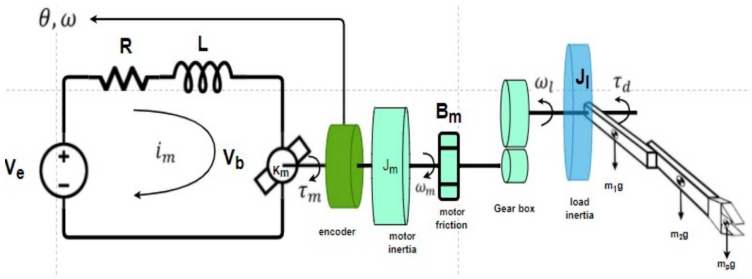

Fig. 1. Proposed dynamical system with motor at each joint connected to a robot through a gearbox.

to improve robot manipulator tracking control by ensuring robustness, faster convergence, chattering reduction, and energy efficiency in the presence of external disturbances.

2. Related work

In [10], the second-order sliding mode control (SOSMC) is proposed for rigid robot manipulators, achieving smooth control input and maintaining robustness. However, it demands high control effort, which is undesirable for systems with finite energy sources like electric motors. In [11], the authors describe the implementation of the SOSMC for a 2-*degree of freedom* (DOF) robotic arm, showing superior tracking performance over *proportional–integral–derivative* (PID) control but facing chattering issues and robustness loss during the reaching phase. Article [12] proposes an *adaptive terminal sliding mode controller* (ATSMC) for a 2-link robotic manipulator, emphasizing its quick convergence and chattering reduction. However, their primary focus was tracking performance rather than minimizing control effort. In [13], an adaptive SOSMC was developed to address chattering and ensure robustness against uncertainties without requiring prior knowledge of their upper bounds, yet energy consumption remained unaddressed. Authors of [14] designed *integral sliding mode control* (ISMC) to handle matched and unmatched uncertainties. In [15], the higher-order sliding mode controller is proposed for robot manipulators, eliminating chattering without reducing control effort. In [16], a *state-dependent Riccati equation* (SDRE)-based SOSMC for trajectory tracking is introduced, balancing control effort and performance while ensuring global robustness and fast convergence. The authors of [17] integrated ISMC with LQR optimal control for robotic trajectory tracking, removing the reaching phase to enhance robustness, but they still encountered chattering issues. Finally, in [18], a resilient optimal sliding mode control for MIMO nonlinear systems is proposed, maintaining optimal performance despite uncertainties but not addressing the chattering problem.

These studies reveal gaps in addressing energy efficiency, chattering, and robustness in SOSMC. The proposed optimal second-order sliding mode control aims to fill these gaps by combining input–output linearization for high-speed operation, fast non-singular terminal sliding manifold convergence (NTSMC), and reduced chattering with minimal control energy, ensuring high robustness and tracking performance.

3. Materials and methods

3.1. Mathematical model

The mathematical model of the manipulator dynamics is a fundamental step for the control design and simulation of the manipulator's motion. This preliminary step is essential to verify the performance of the control scheme before it is used in actual robotic applications. In this research, the Euler–Lagrange formulation is used to determine the dynamic model of an n-DOF robotic arm. This approach is chosen for its computational efficiency in deriving the equations and its suitability for any degree of freedom (DOF). The overall governing dynamic equation of the robot's motion, excluding actuator effects, is given by

$$\tau = M(q)\,\ddot{q} + V(q,\dot{q})\,\dot{q} + G(q) + F(\dot{q}) + \tau_d, \qquad (1)$$

where $M(q) \in \mathbb{R}^{2\times 2}$ is an inertia matrix, $V(q,\dot{q}) \in \mathbb{R}^{2\times 2}$ is a Coriolis and centripetal matrices, $G(q) \in \mathbb{R}^{2\times 1}$ is a gravity vector, $F(\dot{q}) \in \mathbb{R}^{2\times 1}$ represents friction term, and τ_d is the exogenous disturbance torque.

The effect of actuator dynamics has been considered, as presented in Fig. 1. The entire dynamic equation of the gear mechanism and DC motors is determined as follows

$$u = i_m R + L\frac{\mathrm{d}i_m}{\mathrm{d}t}, \qquad (2)$$

$$\tau_m = K_m\, i_m, \qquad (3)$$

$$V_b = K_b \dot{\theta}_m, \qquad (4)$$

$$J_m \ddot{\theta}_m + B_m \dot{\theta}_m + \frac{\tau}{G} = \tau_m, \qquad (5)$$

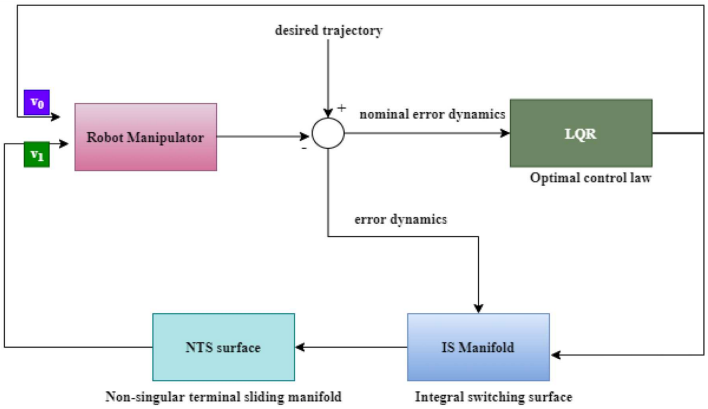

Fig. 2. The OSOSMC control strategy.

where $J_m \in \mathbb{R}^{2\times 2}$ is the motor inertia, $\theta_m \in \mathbb{R}^{2\times 1}$ is the angular position, $B_m \in \mathbb{R}^{2\times 2}$ is the damping constant, $G \in \mathbb{R}^{2\times 2}$ is the gearbox ratio, u is the voltage input, R is the resistance, L is the inductance, i_m is the current, K_m is a motor constant, and K_b is the back-emf constant.

Finally, the dynamics of a robot, including the effects of actuators and gearboxes, can be expressed in a compact form as

$$H\left(q\right)\ddot{q} + N\left(q,\dot{q}\right)\dot{q} + G\left(q\right) + \delta\left(q,\dot{q}\right) = u, \tag{6}$$

where $H(q) = M(q) + G^2 J_m$, $N(q,\dot{q}) = V(q,\dot{q}) + G^2(B_m + K_m K_b/R)$, $\delta(q,\dot{q}) = F(\dot{q}) + \tau_m, u = G\,K_m/R$.

3.2. Controller design

First, a feedback linearization strategy (see Fig. 2) has been applied to (6) to obtain a decoupled and linear model as follows

$$e_i\left(t\right) = y_i\left(t\right) - q_r\left(t\right), \tag{7}$$

$$e_1 = q_1\left(t\right) - r_1\left(t\right), \tag{8}$$

$$\dot{e_1}\left(t\right) = e_3\left(t\right), \tag{9}$$

$$\dot{e_3}\left(t\right) = L_f^2 h_1\left(x\right) + L_{g1}L_f h_1 u_1 + L_{g2}L_f h_1 u_2 - \ddot{r_1}\left(t\right) = v_1, \tag{10}$$

$$\dot{e_4}\left(t\right) = L_f^2 h_2\left(x\right) + L_{g1}L_f h_2 u_1 + L_{g2}L_f h_1 u_2 - \ddot{r_2}\left(t\right) = v_2, \tag{11}$$

where $i = 1,2,3,4$, and the number of the states is $L_f^2 h_i\left(x\right) = -H\left(q\right)^{-1}(N\left(q,\dot{q}\right)\dot{q} + G\left(q\right))$, $L_{g2}L_f h_1 = H\left(q\right)^{-1}$.

Equations (7)–(11) can be represented in state-space form by accounting for various disturbances that impact the system as follows

$$\dot{e}\left(t\right) = A\,e(t) + B\,v(t) + \Delta\left(e,t\right). \tag{12}$$

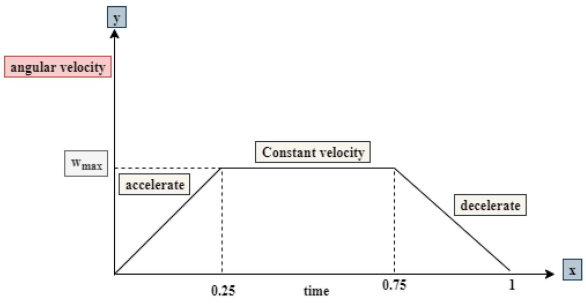

Fig. 3. Trapezoidal velocity profile.

Next, an LQR controller is designed based on the nominal part of the feedback linearized dynamics of the system, ignoring the various disturbances for the time being, as follows

$$\dot{e}\left(t\right) = A\,e(t) + B\,v_0(t). \tag{13}$$

This optimal control problem seeks a control input v_0 that guides the nominal part of the system described in (13) to follow an optimal trajectory $e(t)$, thereby minimizing the cost function

$$J = \frac{1}{2}\int_0^\infty \mathrm{d}t\ \left[e(t)^{\mathrm{T}} Q\,e\left(t\right) + v_0^{\mathrm{T}} R v_0\right], \tag{14}$$

where J is a cost function, Q is a symmetric semi-positive definite matrix, and R is a positive definite matrix, and

$$v_0 = -R^{-1}B^{\mathrm{T}}P\,e(t) = -K\,e(t), \tag{15}$$

where P is a solution of the Riccati equation

$$PA + A^{\mathrm{T}}P - PBR^{-1}B^{\mathrm{T}}P + Q = 0. \tag{16}$$

The optimal control strategy defined in (15) should be integrated with the second-order sliding mode control (SOSMC) as the optimal SOSMC (OSOSMC, see Fig. 3) to ensure that the system tracks the desired trajectory, even in the presence of disturbances, while minimizing control effort. The design of SOSMC controller involves the following two steps [10].

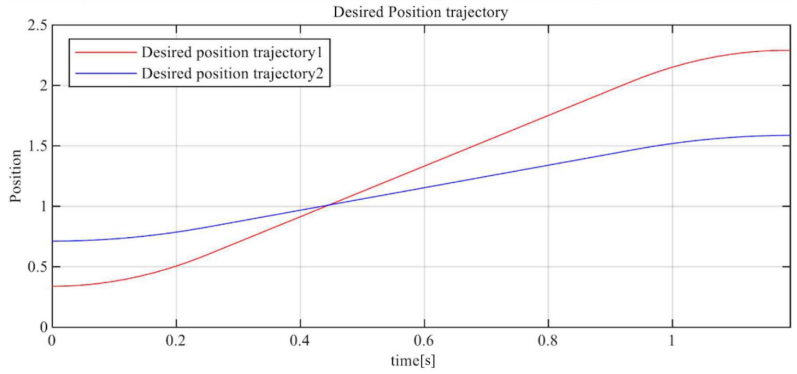

Fig. 4. Desired position trajectory.

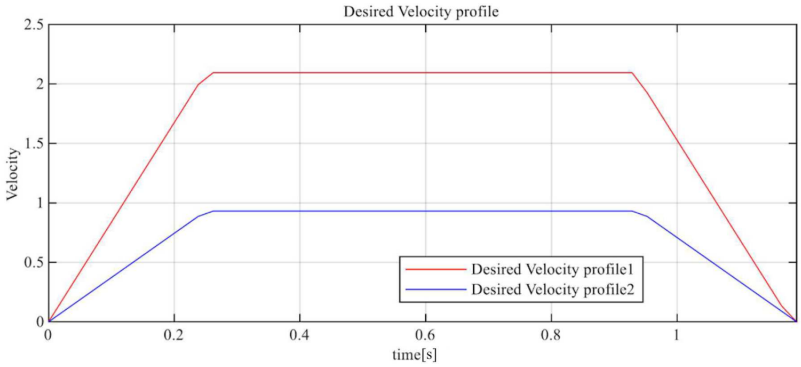

Fig. 5. Desired velocity trajectory.

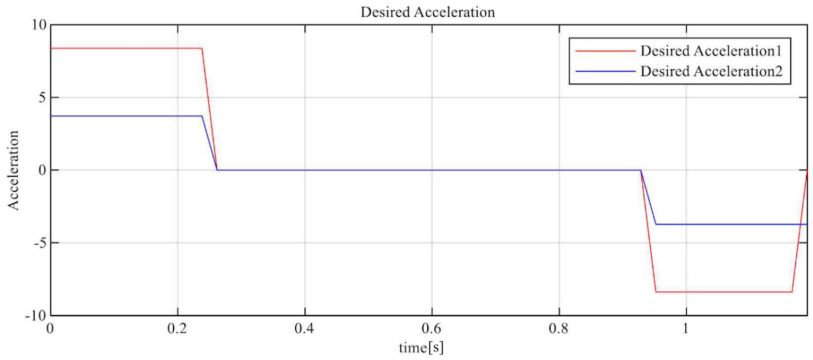

Fig. 6. Desired acceleration trajectory.

Step one: The integral sliding manifold is designed as follows

$$s\left(t\right)=N\left[e(t)-\int_{0}^{t}\mathrm{d}\tau\ \dot{\varphi}\left(t\right)\right], \tag{17}$$

where $N\in\mathbb{R}^{m\times n}$ is a design parameter chosen in such a way that $N\times B$ is invertible and $\varphi(t)=A\,e(t)+B\,v_0(t)$.

Step two: The non-singular terminal sliding mode controller is designed on top of the integral sliding manifold, resulting in a second-order sliding controller. This approach mitigates chattering and ensures convergence to zero in finite time. The non-singular terminal sliding manifold (NSTSM) is defined as

$$\sigma\left(t\right)=s\left(t\right)+\gamma\,\dot{s}\left(t\right)^{\frac{a}{b}}, \tag{18}$$

where γ is NTSM gain, and the values of a and b are chosen as $1<a/b<2$.

Let us differentiate the non-singular terminal sliding surface concerning time as follows

$$\dot{\sigma}\left(t\right)=\dot{s}(t)+\gamma\,\frac{a}{b}\dot{s}(t)^{\frac{a}{b}-1}\,\ddot{s}\left(t\right). \tag{19}$$

The reaching law approach is crucial in designing the control law for SOSMC, and its structure is defined as follows

$$\dot{\sigma}\left(t\right)=-\mu_1\,\mathrm{sgn}\left(\sigma(t)\right)-\mu\,\sigma(t), \tag{20}$$

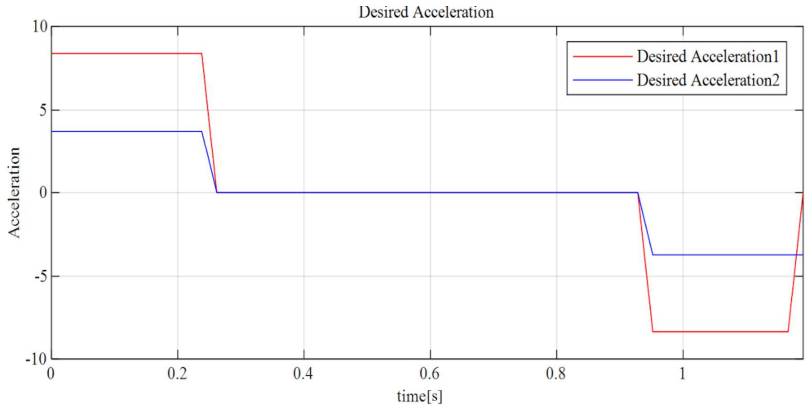

Fig. 7. SimMechanics model of the system.

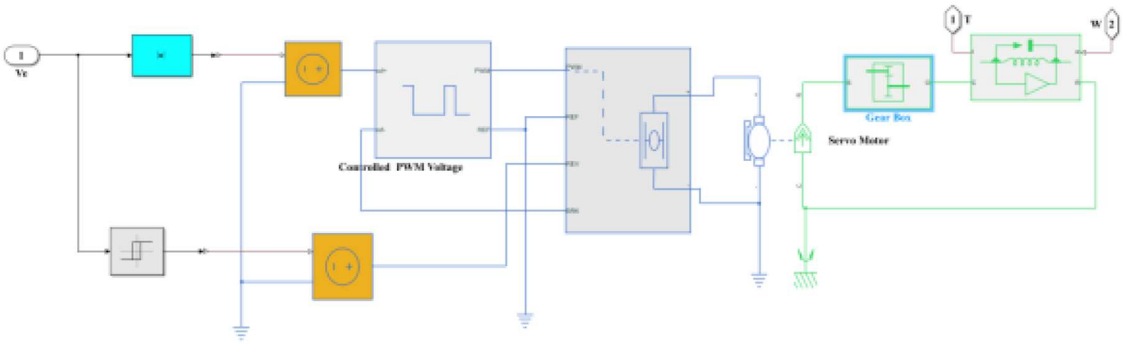

Fig. 8. Motor SimScape model.

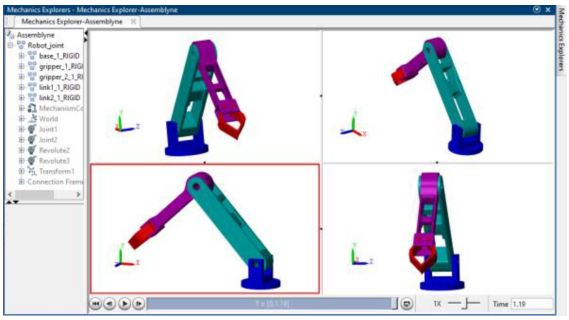

Fig. 9. SimMechanics animation.

where μ_1 is a constant reaching gain and μ is exponential reaching gain.

Then, by equalizing and simplifying equations (19) and (20), we will get

$$\ddot{s}\,(t) = -\mu_0 \operatorname{sgn}(\sigma(t)) - \varepsilon\sigma(t) - \frac{1}{\alpha}\,\dot{s}\,(t)^{-\beta}. \tag{21}$$

Finally, we differentiate equation (17) twice and equate it with (21) to get the switching control as

$$NB\dot{v}_1 + N\dot{\Delta}\,(e,t) = -\mu_0 \operatorname{sgn}(\sigma(t)) - \varepsilon\,\sigma(t) - \frac{1}{\alpha}\,\dot{s}(t)^{-\beta}, \tag{22}$$

$$v_1\,(t) = -\int_0^t \mathrm{d}t\ \left(NB^{-1}\right)\Big[\mu_0 \operatorname{sgn}(\sigma(t)) + \varepsilon\,\sigma(t) + \frac{1}{\alpha}\,\dot{s}\,(t)^{-\beta} + N\dot{\Delta}\,(e,t)\Big]. \tag{23}$$

It is worth noting that integration makes the applied control signal smooth.

3.3. Motor selection

It is essential to calculate the maximum torque to select the appropriate motor for each manipulator joint. It includes both the holding torque (to counteract gravity when the arm is fully extended horizontally) and the acceleration torque (to move the manipulator from rest to the desired speed). The motors experience maximum torque when the arm is fully extended horizontally. The torque at joints 1 and 2 is determined by balancing the torque around a point, as expressed by

$$\tau_H = \sum m_i\, g\, l_i, \tag{24}$$

where m_i is the mass of the i-th link, g is the gravitational constant, and l_i is the length of the i-th link.

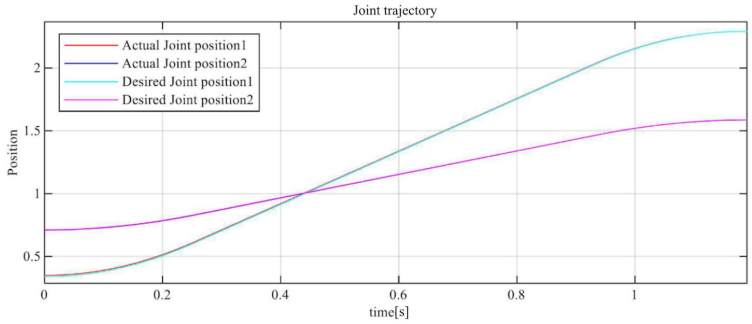

Fig. 10. Position tracking accuracy using OSOSMC.

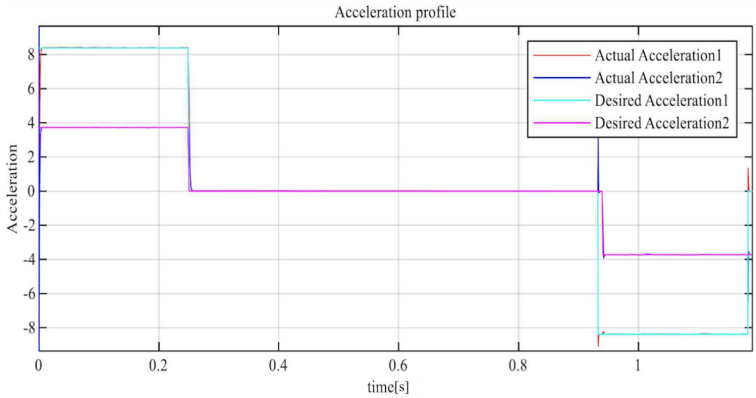

Fig. 11. Acceleration tracking accuracy using OSOSMC.

In addition to holding a position, the manipulator must move within its workspace, which requires an acceleration torque to reach the desired speed, calculated as

$$\tau_a = I\,\alpha. \tag{25}$$

The total torque required to hold a load in a place and to accelerate it for each joint is given as

$$\tau_i = \tau_H + \tau_a. \tag{26}$$

3.4. Trajectory generation

Before implementing a control scheme for a robotic manipulator, it is critical to define the desired trajectory, especially for tasks such as arc welding and assembly. It ensures that the manipulator avoids obstacles and that the path remains within the voltage and torque limits of the actuators. The example trapezoidal path (Fig. 4) is defined as follows

$$q(t) = \begin{cases} q_0 + \dfrac{at^2}{2}, & 0 \le t \le t_a, \\ q_0 + \dot{q}_{\max}\left(t - \dfrac{t_a}{2}\right), & t_a \le t \le t_f - t_a, \\ q_f + \dfrac{\alpha}{2}(t_f - t), & t_f - t_a \le t \le t_f. \end{cases} \tag{27}$$

Figures 4–6 illustrate the desired joint trajectories the manipulator must follow to perform a given task.

4. Result and discussion

In the simulation, the following parameters were used: $a = 5$, $b = 3$, $\mu_0 = 20$, $\varepsilon = 0.5$, $\alpha = 0.4$, $G = 100$, $K_m = 1.4$, $K_b = 0.82$, $\tau_{\max} = 21N$, $\omega_{\max} = 2000$ rpm, $J_m = 4.8 \times 10^{-4}$, and

$$N = \begin{bmatrix} 2 & 2 & 2 & 1 \\ 2 & 2 & 1 & 2 \end{bmatrix}. \tag{28}$$

Figures 7–9 illustrate the SimScape models of a robot and its corresponding joint motors. This approach ensures that the controller optimized in SimMechanics remains effective for the actual system, thanks to the realistic modeling of physical factors.

Figures 10–11 show that each joint position of the manipulator successfully follows the desired trajectory, with both joints perfectly tracking the specified path by implementing the proposed optimal second-order sliding mode control (OSOSMC) scheme. It confirms that OSOSMC is effective in ensuring high tracking performance.

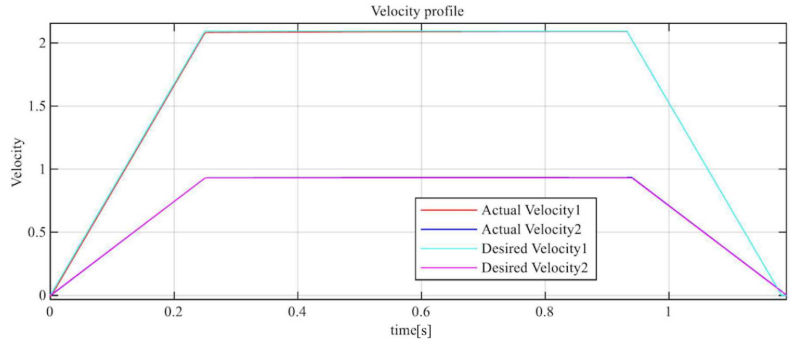

Fig. 12. Velocity tracking accuracy using OSOSMC.

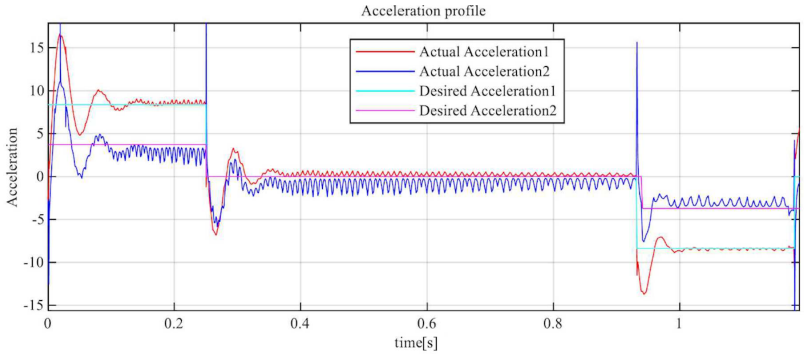

Fig. 13. Acceleration profile using OSMC.

TABLE I

Comparison of accuracy and energy consumption of different SMC-based control strategies.

Controller	IAE			Energy
		joint 1	joint 2	
OSOSMC	position	0.0082	0.0017	27.63
	velocity	0.0083	0.0040	
		joint 1	joint 2	
OSMC	position	0.0572	0.0386	30.87
	velocity	0.1048	0.0952	

As shown in Fig. 12, each joint of the manipulator precisely tracks even the sharp corners, demonstrating the effectiveness and efficiency of the control law. This velocity profile is designed by balancing speed and acceleration.

Each joint of the robot arm closely follows the corresponding desired trajectories, with only a small overshoot during the transition to the deceleration phase. However, a high-frequency chatter phenomenon in the acceleration profile (Fig. 13) degrades tracking accuracy. This problem arises because the switching function is applied directly to the control input, and the angular acceleration is directly proportional to the torque applied to each joint.

Simulation results show OSOSMC's superiority over similar strategies as presented in Table I, offering exceptional energy efficiency and accurate tracking, while significantly reducing chattering in the control signal. This reduction is crucial as it minimizes wear on the manipulator's components, extending its lifespan. Although OSMC effectively tracks the target trajectory despite external disturbances, its switching component introduces chattering, which can damage moving components and increase the overall system costs by reducing actuator lifespan. This makes OSMC less suitable for real-world applications.

5. Conclusions

The proposed optimal second-order sliding mode control (OSOSMC) law was successfully implemented in the manipulator SimMechanics model, demonstrating its effectiveness. OSOSMC provides robust and precise tracking control, making it ideal for industrial robot manipulators in harsh environments where precision, durability, and efficiency are critical. The modular design of the proposed control strategy enables scalability to more complex multi-degree-of-freedom (DOF) systems, efficiently handling increased joint coupling and nonlinearities.

This ensures optimal performance and robustness in high-dimensional robotic systems, such as multi-link manipulators or humanoid robots, where traditional control approaches may struggle. The main challenge in OSOSMC design lies in tuning numerous parameters to meet specifications, which suggests that modern optimization techniques like particle swarm optimization (PSO) should be considered for future work.

References

[1] J. Iqbal, R.U. Islam, S.Z. Abbas, A.A. Khan, S.A. Ajwad, *Teh. Vjesn.* **23**, 917 (2016).

[2] N.M.H. Norsahperi, K.A. Danapalasingam, *Int. J. Electr. Comput. Eng. Syst.* **10**, 73 (2019).

[3] N.M.H. Norsahperi, K.A. Danapalasingam, *Mech. Syst. Signal Process.* **142**, 106747 (2020).

[4] S. Tayebi-Haghighi, F. Piltan, J.-M. Kim, *Robotics* **7**, 13 (2018).

[5] J. Baek, W. Kwon, *Appl. Sci.* **10**, 2909 (2020).

[6] A.Q. Al-Dujaili, A. Falah, A.J. Humaidi, D.A. Pereira, I.K. Ibraheem, *Int. J. Adv. Robot. Syst.* **17**, 1 (2020).

[7] W.M. Elawady, Y. Bouteraa, A. Elmogy, *Robotics* **9**, 1 (2020).

[8] İ.Ö. Bucak, in: *Automation and Control*, Eds. C. Volosencu, S. Küçük, J. Guerrero, O. Valero, IntechOpen 2021.

[9] A. Ferrara, L. Magnani, *J. Intell. Robot. Syst. Theory Appl.* **48**, 23 (2007).

[10] L.M. Capisani, A. Ferrara, L. Magnani, in: *Proc. IEEE Conf. Decis. Control*, 2007, p. 3691.

[11] K. Dumlu, *J. Inst. Sci. Technol.* **8**, 77 (2018).

[12] S. Chanda, P. Gogoi, *J. Sci. Eng. Res.* **2**, 18 (2014).

[13] S. Mondal, Ph.D. Thesis, Indian Institute of Technology Guwahati, 2012.

[14] F. Castaños, L. Fridman, *IEEE Trans. Automat. Contr.* **51**, 853 (2006).

[15] N. Mezghani Ben Romdhane, T. Damak in: *Studies in Computational Intelligence*, Vol. 576, Eds. A. Azar, Q. Zhu, Springer, Cham 2015 p. 327.

[16] H.R. Shafei, M. Bahrami, H.A. Talebi, *J. Brazilian Soc. Mech. Sci. Eng.* **42**, 301 (2020).

[17] W. Boukadida, A. Benamor, H. Messaoud, P. Siarry, *Aerosp. Sci. Technol.* **91**, 442 (2019).

[18] H. Pang, X. Yang, *J. Appl. Math.* **2013**, 863168 (2013).